0090-9556/06/3406-961–970$20.00
DRUG METABOLISM AND DISPOSITION
Vol. 34, No. 6
7500/3115193
DMD 34:961–970, 2006
Printed in U.S.A.

METABOLISM OF [^{14}C]GEMOPATRILAT AFTER ORAL ADMINISTRATION TO RATS, DOGS, AND HUMANS

Jill C. M. Wait,[1] Nimish Vaccharajani, James Mitroka, Mohammed Jemal, Sanaullah Khan, Samuel J. Bonacorsi, J. Kent Rinehart, and Ramaswamy A. Iyer

Departments of Biotransformation (J.C.M.W., R.A.I.), Metabolism and Pharmacokinetics (J.M.), Bioanalytical and Discovery Analytical Sciences (M.J., S.K.), Clinical Discovery (N.V.), and Chemical Synthesis (S.J.B., J.K.R.), Bristol-Myers Pharmaceutical Research Institute, Princeton, New Jersey

Received September 19, 2005; accepted March 7, 2006

ABSTRACT:

This study describes the pharmacokinetic parameters of gemopatrilat, a potent vasopeptidase inhibitor, in humans and the comparative biotransformation of the compound in rats, dogs, and humans after administration of a single oral dose of [^{14}C]gemopatrilat. Gemopatrilat was rapidly absorbed in humans with an oral bioavailability of 49%. Within 5 h after dose, the mean concentrations of gemopatrilat were less than 1% of the mean C_{max} values. The total area under the first-moment time curve extrapolated to infinity [AUC(INF)] value for gemopatrilat was only 2% of the AUC(INF) of radioactivity in plasma. Gemopatrilat showed a large apparent steady-state volume of distribution (2500 liters) and a prolonged terminal-phase decline in plasma concentration. These results are consistent with the idea that the free sulfhydryl group of gemopatrilat forms reversible disulfide linkages with plasma and tissue proteins and is thus eliminated from the body at a very slow rate. Approximately half of the drug-related radioactivity in 1-h plasma samples from rat, dog, and human was reduced chemically with dithiothreitol to gemopatrilat, suggesting that disulfide linkage occurred in all species. In addition, metabolites formed through *S*-methylation and amide hydrolysis were also detected in rat, dog, and human plasma. No gemopatrilat was detected in urine and fecal samples from all three species, indicating that the compound is extensively metabolized in vivo. The major metabolites identified in human urine and feces were also present in rat and dog. These data suggest that the metabolism of gemopatrilat in all three species were qualitatively very similar.

Gemopatrilat is a potent vasopeptidase inhibitor that inhibits two key enzymes involved in the regulation of cardiovascular function: neutral endopeptidase (NEP) and angiotensin-converting enzyme (ACE) (Robl et al., 1999; Hubner et al., 2001; Singh et al., 2003). ACE and NEP are zinc metalloproteases that catalyze the conversion of angiotensin I to angiotensin II (AII) and degradation of atrial natriuretic peptide (ANP), respectively (Burnett, 1999). AII, a potent vasoconstrictor, triggers the release of aldosterone, a sodium-retaining steroid, that leads to elevated blood pressure, causing an increase in both vascular resistance and fluid volume (Trippodo et al., 1995). Whereas ANP, secreted by the heart in response to atrial distention, by interaction with its receptor promotes the generation of cyclic guanosine monophosphate (cGMP), resulting in vasodilation, natriuresis, diuresis, and possibly inhibition of aldosterone formation. ANP has an opposite effect to that of AII (Seymour et al., 1995; Trippodo et al., 1995). Gemopatrilat, as a potent inhibitor of both ACE and NEP, offers several advantages over existing ACE inhibitors (Sagnella, 2002).

Gemopatrilat is structurally related to omapatrilat, both containing the sulfhydryl group needed for binding to zinc in the active site of ACE and NEP (Delaney et al., 1994). Studies on the metabolism of omapatrilat in rat, dog, and humans have been conducted and reported (Iyer et al., 2001, 2003). The metabolic pathways identified for omapatrilat included methylation and disulfide conjugation at the free thiol group, glucuronide conjugation of the carboxyl group, oxidation of the *S*-methyl metabolite, and hydrolysis of the exocyclic amide bond. The present in vivo studies, conducted with a mixture of [^{14}C]gemopatrilat labeled at either the exocyclic carbonyl carbon or the gem-dimethyl groups (Fig. 1), describe the comparative biotransformation of gemopatrilat in rats, dogs, and humans. Rats and dogs were the species used for long-term toxicity testing in the development of gemopatrilat.

Materials and Methods

Chemicals. The reference standards for HPLC, namely (*S*)-3-aminohexahydro-7,7-dimethyl-2-oxo-1*H*-azepine-1-acetic acid (amine-side hydrolysis product of gemopatrilat), (*S*)-3-(acetylamino)hexahydro-7,7-dimethyl-2-oxo-1*H*-azepine-1-acetic acid (*N*-acetyl derivative of the amine-side hydrolysis product of gemopatrilat), diastereomeric sulfoxides of (*S*)-2-thiomethyl-3-phenylpropionic acid, L-cysteine mixed disulfide of gemopatrilat, diastereomeric sulfoxides of *S*-methyl gemopatrilat, (*S*)-2-thio-3-phenylpropionic acid,

This work was previously presented as a poster at the 11th North American International Society for the Study of Xenobiotics meeting; Oct 27–31, 2002; Orlando, FL.

[1] Current affiliation: Pharmacokinetics and Drug Metabolism, Amgen, South San Francisco, CA.Article, publication date, and citation information can be found at http://dmd.aspetjournals.org.

doi:10.1124/dmd.105.007500.

ABBREVIATIONS: NEP, neutral endopeptidase; ACE, angiotensin-converting enzyme; AII, angiotensin II; ANP, atrial natriuretic peptide; HPLC, high-performance liquid chromatography; TLC, thin layer chromatography; LC/MS, liquid chromatography/mass spectrometry; LSC, liquid scintillation counting; MS/MS, tandem mass spectrometry; QC, quality control; AUC, area under the curve; DTT, dithiothreitol.

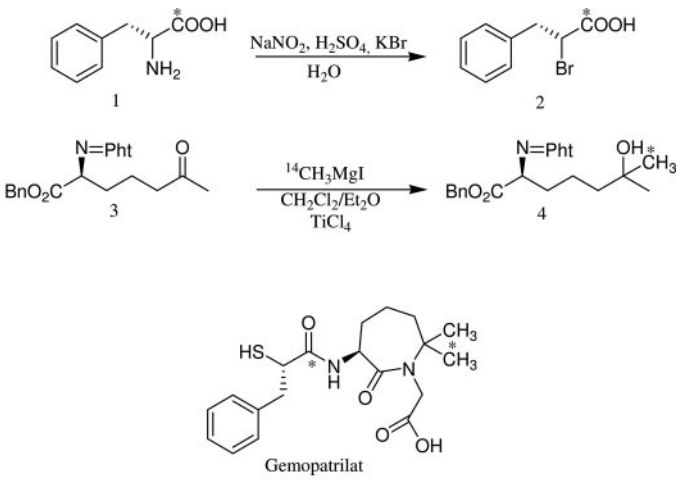

* Denotes the position of the C-14 label. The C-14 label could be on any one of the two methyl groups. In a single molecule both the methyl groups are not labeled.

FIG. 1. Structures of [^{14}C]gemopatrilat and its C-14-labeled synthetic starting material. The site labeled with ^{14}C is indicated with an asterisk.

(*S*)-2-thiomethyl-3-phenylpropionic acid, gemopatrilat, *S*-methyl gemopatrilat, and symmetrical disulfide of gemopatrilat were obtained from Research Chemical Distribution, Bristol-Myers Squibb Pharmaceutical Institute. [^{14}C]Gemopatrilat with C-14 label on the exocyclic carbonyl carbon (10.4 μCi/mg, radiochemical purity 99.5%) and [^{14}C]gemopatrilat with C-14 label on one of the gem-dimethyl carbon on the bicyclic ring (10.3 μCi/mg, radiochemical purity 98.4%) (see Fig. 1) were provided by the Radiochemistry Group, Department of Discovery Chemistry, Princeton, NJ. The radiolabeled precursors $^{14}CH_3I$ and D-phenylalanine-[1-^{14}C] were obtained from Amersham Life Sciences, Piscataway, NJ. Ecolite liquid scintillation cocktail was purchased from ICN Biomedicals, Inc., Costa Mesa, CA. β-Glucuronidase from *Helix pomatia* and D-saccharic acid 1,4-lactone were obtained from Sigma Chemical Co., St. Louis, MO. For solid-phase extraction, Sep-Pak Vac 20.0 cc (C-18, 5.0 g) cartridges were obtained from Waters Corporation, Milford, MA. All other chemicals used were reagent grade or better.

Synthesis of [^{14}C]Gemopatrilat. Synthesis of gem-dimethyl and exocyclic carbonyl carbon-labeled [^{14}C]gemopatrilat was accomplished from their C-14-labeled precursors (Fig. 1). The remaining steps for the synthesis of [^{14}C]gemopatrilat were accomplished with synthetic procedures outlined in two articles (Robl et al., 1999; Singh et al., 2003). Here, we only describe the procedures used for the synthesis of the C-14-labeled precursors.

Preparation of C-14-Labeled (*S*)-2-Phthalimido-6-Methyl-6-Hydroxyheptanoic Acid Phenylmethyl Ester (4). An ampoule containing $^{14}CH_3I$ (100 mCi, 257 mg, 1.78 mmol) was attached to a vacuum line and its contents transferred to a cooled receiver. The $^{14}CH_3I$ was then diluted with anhydrous ether (2× 10 ml) and transferred by syringe using a three-way valve to a 50-ml dropping funnel. Once transferred, methyl iodide (1.60 g, 13.10 mmol) was added to the ethereal solution. The contents of the funnel were mixed by gentle swirling. The funnel was then attached to a 250-ml flask equipped with a dry ice/acetone condenser containing magnesium turnings and 10 ml of anhydrous ether. The flask contents were stirred together with a chip of iodine for 1 h before the addition of $^{14}CH_3I$, which was performed drop-wise over 20 min. After the addition, the dropping funnel was rinsed with 5 ml of ether and the reaction stirred for 1 h. The dropping funnel was then charged with 1.0 M $TiCl_4$ in CH_2Cl_2 (13.1 ml, 13.1 mmol). The reaction flask was cooled to −40°C, and the $TiCl_4$ solution was added to the Gringard reagent drop-wise over a 10-min period. Stirring was maintained for an additional 30 min. (*S*)-2-Phthalimido-6-ketoheptane phenylmethyl ester (19.79 ml of a 0.662 M solution in CH_2Cl_2, 13.1 mmol) was added rapidly (5 min) from the dropping funnel to the cooled (−40°C) reaction mixture. After 15 min, the reaction was warmed to 0°C and stirred for 2.5 h. The work-up involved quenching the reaction with an aqueous solution of saturated NH_4Cl (100 ml) and extracting with CH_2Cl_2 (50 ml × 2). The organic extracts were combined and washed with brine (25 ml), dried over anhydrous $MgSO_4$, filtered, and concentrated in vacuo to give a crude black oil. The oil was chromatographed on 600 ml of silica gel eluting with 70:30 hexane/ethyl acetate. Final purification gave a TLC homogeneous compound weighing 2.93 g (57%) with a specific activity of 15.1 μCi/mg; TLC: R_f = 0.1 (80:20 hexane/ethyl acetate); ^{1}H NMR (300 MHz) and ^{13}C NMR (100 MHz) were consistent with the published structure (Robl et al., 1999).

Preparation of D-Phenyl-2-Bromopropionic-[1-^{14}C] Acid (2). D-Phenylalanine-[1-^{14}C] (73.2 mg, 25 mCi) was combined with nonlabeled D-phenylalanine (1023 mg) (total 1096.2 mg, 6.63 mmol). Potassium bromide (2.76 g, 23.21 mmol) was added, and the solid was dissolved in 3.0 N H_2SO_4 (10 ml). The resulting solution was cooled to −15°C, and a solution containing $NaNO_2$ (0.709 g, 10.3 mmol) in 3.0 ml of water was added drop-wise over 20 min. The reaction mixture was stirred at −10°C for 2 h. The reaction mixture was then warmed to room temperature and extracted with CH_2Cl_2 (3 × 30 ml). The solution was dried over Na_2SO_4, filtered, and concentrated to an oil weighing 1.539 g (99%). The crude product was used without purification in the next step; TLC: R_f = 0.6 (90:10 CH_2Cl_2-CH_3OH); ^{1}H NMR ($CDCl_3$, 300 MHz) δ 3.3 (dd, 2H), 4.4 (t, 1H), 7.2 (m, 5H), 8.8 (s, 1H).

Dosing and Sample Collection. Samples of urine, feces, and plasma were obtained from studies in which single oral doses of [^{14}C]gemopatrilat (equal portions of exocyclic carbonyl carbon and gem-dimethyl group-labeled compound) were administered to male Sprague-Dawley rats (50 mg/kg, 0.8 μCi/mg), male beagle dogs (100 mg, 50 μCi), and from a crossover study in healthy human subjects given oral (50 mg, 112 μCi) and i.v. (20 mg, 100 μCi) doses. Blood samples from the human study for the determination of plasma concentrations of radioactivity and unchanged gemopatrilat were collected at serial time points up to 120 and 168 h after dose after oral and i.v. administration, respectively. For biotransformation analysis, additional blood samples were collected at 1 and 6 h after dose from rat, dog, and human study. All blood samples for determination of radioactivity (human) and biotransformation analysis were collected into Vacutainer tubes containing ethylenediaminetetraacetic acid (EDTA) as an anticoagulant without methyl acrylate. The pharmacokinetic blood samples for determination of unchanged gemopatrilat were collected into EDTA Vacutainer tubes that also contained methyl acrylate (10 μl per ml of blood). Methyl acrylate was used to form a Michael adduct with the sulfhydryl group of gemopatrilat and its metabolites similar to the procedure developed for omapatrilat (Jemal and Hawthorne, 1997a,b). Plasma was prepared from the blood samples by centrifuging for 15 min at 1000*g* and 5°C. Urine and feces was collected from rats, dogs, and humans at 24-h intervals for the duration of the study. All urine samples were collected over acetic acid to give a final pH between 4 and 5. The volume of acetic acid added to each collection container was 0.5 ml (20-ml container), 2 ml (0.5-liter container), and 2.5 ml (1-liter container) for rat, dog, and human, respectively. This was done to stabilize the acyl glucuronides in urine samples.

Representative pooled urine and fecal samples were prepared by combining a constant percentage of urine volume or fecal homogenate by weight across animals or subjects. Pooled samples from 0 to 24 h for rat, 0 to 48 h for dog, and 0 to 168 h for human were used for radioactivity profiling. Pooled samples of 0 to 24-h human urine were used for LC/MS analysis. Plasma samples were segregated by collection time (1 and 6 h), and equal volumes of plasma were combined from each subject. All samples for gemopatrilat assay in plasma and for biotransformation analyses in plasma and urine were stored at −70°C, and those for radioactivity assay in plasma were stored at −20°C until the time of analysis.

Analyses of Radioactivity. Samples of plasma and urine, in duplicate, were mixed with 15 ml of Hionic-Fluor scintillation cocktail for the analysis of radioactivity by liquid scintillation counting (LSC), respectively. The fecal samples were transferred to tared containers and homogenized with water. The weight of the fecal homogenate was recorded for each sample. Accurately weighed duplicate 0.2-g portions of the fecal homogenates were combusted to $^{14}CO_2$. Blood samples (0.2 ml each) were directly combusted to $^{14}CO_2$. Combustion of the blood and fecal samples was carried out in a model 307 automated sample oxidizer (Packard Instrument Company, Meriden, CT), and the $^{14}CO_2$ was trapped in 8 ml of Carbo-Sorb. Perma-Fluor scintillation cocktail (9 ml) was added to the $^{14}CO_2$-containing Carbo-Sorb sample. C-14-labeled standards prepared in blank fecal matrix were combusted along with the study samples to determine combustion efficiency.

Radioactivity in all samples in duplicate was determined by LSC in a model Tri-Carb-2750TR/LL liquid scintillation spectrophotometer (Packard Instrument Company) equipped with automatic background subtraction and quench correction. All samples were counted for 20 min each or to a 2% 2-sigma error. The lower limit of quantitation, based on a 20% coefficient of variation for the acceptable limit of error in the determination of radioactivity, was 10 ng-equivalent of gemopatrilat per milliliter of the plasma and urine samples or per gram of fecal samples.

Analysis of Gemopatrilat. The plasma concentrations of unchanged gemopatrilat, measured as its methylacrylate adduct in human plasma, were determined by a validated LC/MS/MS method similar to the one used for analysis of omapatrilat in human plasma (Jemal et al., 2001). The internal standard used for analysis was d_5-gemopatrilat. The standard curve ranges in plasma were 0.5 to 500 ng/ml. Quality control (QC) samples were included in each analytical run. Deviations of the predicted concentrations for at least two-thirds of the QC samples were within ±15% of their nominal values at all concentration levels. The between-run and within-run variability estimates for the analytical QC samples were no greater than 15 to 20% CV at the lowest QC concentration and 10% CV at the higher QC concentrations. These data are indicative of accuracy and precision in the analysis of gemopatrilat in plasma.

Pharmacokinetic Analysis Methods. The plasma concentration versus time data for gemopatrilat and radioactivity, respectively, were analyzed by a noncompartmental method. The peak plasma concentration C_{max} and the time to reach peak concentration T_{max} were recorded directly from experimental observations. The area under the plasma concentration versus time curve (AUC) was calculated by a combination of trapezoidal and log-trapezoidal methods. The AUC was calculated from time 0 to the time, T, of last measurable concentration [AUC(0-T)]. The first-order rate constant of decline of concentrations in the terminal phase of each plasma concentration versus time profile, K, was estimated by log-linear regression (using no weighting factor) of at least three data points that yielded a minimum mean square error. The absolute value of K was used to estimate the apparent terminal elimination half-life T-HALF. To estimate AUC(INF), the last measurable concentration and the rate constant K were used to extrapolate AUC(0-T) to infinity. The total body clearance (CLT) of gemopatrilat was calculated as the ratio of intravenous dose and AUC(INF). The mean residence time [MRT(INF)] was calculated using the following equation, where the infusion time equals 0.5 h.

$$\mathrm{MRT(INF)} = \{\mathrm{AUMC(INF)/AUC(INF)}\} - \{\mathrm{Infusion\ Time/2}\}$$

where AUMC(INF) is the total area under the first-moment time curve extrapolated to infinity. The steady-state volume of distribution, VSS, of gemopatrilat was calculated using the following equation.

$$\mathrm{VSS} = \mathrm{CLT} \cdot \mathrm{MRT} = \{\mathrm{Dose} \cdot \mathrm{AUMC(INF)}/(\mathrm{AUC(INF)})^2\} - \{(\mathrm{Dose/AUC(INF)}) \cdot (\mathrm{Infusion\ Time}/2)\}$$

The absolute bioavailability (F) of gemopatrilat was calculated as the ratio of dose-normalized AUC(INF) values of gemopatrilat determined after oral dose to that after intravenous dose.

The amount of radioactivity eliminated in the urine or feces was determined as the product of radioactivity concentration and the total volume or weight collected at each interval. Total urinary (%Urine) or fecal (%Feces) recovery was calculated as the cumulative amount excreted over 168 h and was expressed as the percentage of the administered oral dose.

Preparation of Samples for Radioactivity Profiling. *Plasma.* The 1-h pooled plasma volume used for analysis from rat, dog, and human ranged between 1.2 and 2.0 ml. Pooled plasma was extracted by a procedure previously published by this laboratory (Iyer et al., 2001, 2003). Dithiothreitol (DTT) reduction of plasma sample was done by incubating 0.5 ml of plasma with 1.0 ml of 0.2 M DTT solution in water at 37°C for 1 h. The plasma samples were then extracted in a similar manner as described above.

Urine. Pooled rat and dog urine was centrifuged at 14,200*g* for 10 min and injected (40 μl) onto the HPLC for profiling. For profiling of pooled human 0 to 168-h urine samples, 0.5 ml of the urine was evaporated to dryness. The residue was suspended in 0.1 ml of 50% methanol and 50% water and centrifuged at 14,200*g* for 10 min. The supernatant (50 μl) was injected onto the HPLC.

Feces. The fecal homogenate aliquot used for analysis from rat, dog, and human was 0.23, 5.0, and 5.0 g, respectively. Each pooled fecal homogenate was extracted by addition of 2 volumes of acetonitrile to 1 volume of fecal homogenate and mixed on a Vortex mixer. The mixture was sonicated for 5 min and then centrifuged at 1900*g* for 5 min. The supernatant was removed and saved. The extraction was repeated two times, and the supernatants were combined and evaporated to dryness on a Savant Speed-Vac. The residue was suspended in 0.5 ml of the HPLC solvent system (95% A and 5% B) used for biotransformation analysis and centrifuged at 14,200*g* for 10 min. The supernatant was injected onto the HPLC. A portion of the extracted feces (50 μl) was counted on the LSC to determine the recovery of radioactivity.

β-Glucuronidase/Sulfatase Incubation of Human Urine. Pooled human urine (0–24 h) was treated with β-glucuronidase/sulfatase and DTT under two different conditions. In one set of conditions, pooled human urine (0–24 h) was subjected to β-glucuronidase hydrolysis, with the procedure previously published by this laboratory (Iyer et al., 2001). After β-glucuronidase hydrolysis, the urine samples were divided into two portions. One portion was centrifuged at 14,200*g* for 10 min and injected (50 μl) onto the HPLC. To the other portion, an equal volume of 0.4 M DTT solution in water was added and incubated for 1 h at 37°C. The DTT-treated urine samples were centrifuged at 14,200*g* for 10 min and injected (50 μl) onto the HPLC.

In the second set of conditions, 0 to 24-h human urine (0.5 ml) was treated with 0.5 ml of 0.4 M DTT at 37°C for 1 h. The urine samples treated with DTT were divided into two portions. One portion was centrifuged at 14,200*g* for 10 min and injected (50 μl) onto the HPLC. The other portion was loaded onto an Oasis HLB 1 cc (C-18, 30 mg; Waters) cartridge. The column was washed sequentially with water (1 ml), water containing 0.4% formic acid, and 0.1% triethylamine (pH 2.6, 1 ml) and methanol (1 ml). The radioactivity was quantitatively recovered in the methanol fraction. The methanol fraction was evaporated to dryness under a stream of nitrogen. The residue was suspended in water (150 μl) containing 0.2 M sodium acetate buffer (200 μl, pH 4.8) and a solution of β-glucuronidase (50 μl) in water. The mixture was incubated at 37°C in a water bath for 18 h. The treated urine was centrifuged at 14,200*g* for 10 min and injected (50 μl) onto the HPLC.

HPLC for Biotransformation Analysis. For radioactivity profiling, HPLC was performed on a Shimadzu Class VP system equipped with two pumps (model LC-10AT), an autoinjector (SIL 10AD), and a diode array detector (SPD-M10A) (Shimadzu, Kyoto, Japan). The HPLC column was enclosed in an Eppendorf CH-30 column heater and maintained at 35°C with an Eppendorf TC-45 temperature controller. The solvent systems used consisted of solvent A, water containing 0.4% formic acid, and 0.1% triethylamine (pH 2.6); and solvent B, acetonitrile/water (90:10) containing 0.4% formic acid and 0.1% triethylamine. Profiling of radioactivity was done at a flow rate of 1.0 ml/min with a Zorbax RX C-18 column (4.6 × 250 mm, 5-μ; Agilent Technologies, Wilmington, DE). Solvent B was maintained at 0% for 5 min and then increased linearly between time intervals: 25% (15 min), 30% (30 min), 33% (45 min), 55% (50 min), and 90% (60 min). After sample injection, the HPLC effluent was collected as 15-s fractions on 96-well Packard Lumaplates with a Gilson Model FC 204 fraction collector (Gilson, Middleton, WI). Each fraction of column eluent was evaporated to dryness on a Savant Speed-Vac (Savant Instruments Inc., Holbrook, NY) and counted for radioactivity with a Packard Top Count microplate scintillation analyzer (Packard Biosciences, Downers Grove, IL). For each injection, the average background cpm value was subtracted from the cpm value of each subsequent fraction. Biotransformation profiles were prepared by plotting the resulting net cpm values against time-after-injection. Radioactivity peaks in the biotransformation profiles were reported as a percentage of the total radioactivity collected during the entire HPLC run.

LC/MS and LC/MS/MS Analysis. Two LC/MS systems were used for analysis of urine and fecal samples. One LC/MS system was a Waters Alliance 2690 HPLC equipped with a Waters 996 photodiode array detector and connected to a Finnegan LCQ mass spectrometer. The other LC/MS system was a Shimadzu Class VP HPLC equipped with two pumps (model LC-10AT), an autoinjector (SIL-10AD), and a photodiode array detector (SPD-M10A) and connected to a Finnegan LCQ-Deca XP mass spectrometer. A YMC ODS-AQ C-18 3-μ column (3 × 150 mm) equipped with a guard column was used. The HPLC solvent system used for analysis was the same system used above for biotransformation analysis. The flow rate was 0.43 ml/min.

Mass spectral analysis of all standards and metabolites was performed on a Finnegan LCQ or LCQ-Deca XP mass spectrometer with an electrospray ionization probe. Samples were analyzed in the negative and positive ion mode. For samples introduced by HPLC, the eluent from the HPLC was directed to the Finnegan LCQ mass spectrometer through a divert valve set to divert the flow from 0 to 4 min. From 4 min until the end of the HPLC run, the eluent flow was directed to the mass spectrometer. The capillary temperature used for analysis was 225 and 300°C for the LCQ and LCQ-Deca XP mass spectrometers, respectively. The nitrogen gas flow rate, spray current, and voltages were adjusted to give maximum sensitivity.

LC/MS and LC/MS/MS analyses were done on pooled rat (0–24 h) and dog (0–48 h) urine and fecal samples prepared above. For LC/MS and LC/MS/MS analyses of pooled 0 to 24-h human urine, 100 ml of the urine was concentrated by loading onto an Oasis HLB 35 cc (C-18, 6.0 g) cartridge. The column was washed sequentially with water containing 0.4% formic acid and 0.1% triethylamine (pH 2.6) (4× 10 ml) and methanol (5× 10 ml). The radioactivity was quantitatively recovered in the methanol fractions. The methanol fractions were combined and concentrated under a stream of nitrogen and evaporated to dryness on a Savant Speed-Vac. The residue was suspended in 1 ml of HPLC solvent system (50% A and 50% B) and centrifuged at 14,200*g* for 10 min. An aliquot (10 μl) was injected onto the HPLC. LC/MS and LC/MS/MS analyses were also done on pooled human (0–168 h) fecal samples prepared above.

Results

Synthesis of [^{14}C]Gemopatrilat. The synthesis of [^{14}C]gemopatrilat (gem-dimethyl label) was accomplished in a multistep fashion from the reaction between protected (*S*)-2-amino-6-ketoheptanoic acid and [^{14}C]methylmagnesium iodide (Fig. 1). This gave a radiolabeled carbinol that was converted to its azide and reduced catalytically with hydrogen and palladium on carbon (Robl et al., 1999). The resulting amine was cyclized in situ giving the desired caprolactam with [^{14}C] labeling in the gem-dimethyl group. The azepinone was protected, and the amide linkage alkylated with ethylbromoacetate (Robl et al., 1999). After deprotection, the structural skeleton of [^{14}C]gemopatrilat was prepared by a carbodiimide-mediated coupling between the thioacetate derivative of D-phenylalanine and the radiolabeled azepinone (Singh et al., 2003). Base-promoted hydrolysis of the penultimate ester gave [^{14}C]gemopatrilat in a 25% overall radiochemical yield.

Exocyclic carbonyl-labeled [^{14}C]gemopatrilat was prepared with D-phenylalanine-[1-^{14}C] as the radiolabeled starting material. D-Phenylalanine-[1-^{14}C] was converted to the α-bromophenylpropionic acid precursor with an overall retention of configuration (Yang et al., 2001) (Fig. 1), which was then converted to (2*S*)-[1-^{14}C]-2-thioacetyl-3-phenyl-propanoic acid (Singh et al., 2003). Hydrolysis of the ester functionalities, after coupling of (2*S*)-[1-^{14}C]-2-thioacetyl-3-phenylpropanoic acid with the nonlabeled lactam (Singh et al., 2003), gave the exocyclic carbonyl-labeled [^{14}C]gemopatrilat in an overall yield of 7% from D-phenylalanine-[1-^{14}C].

Pharmacokinetics of Gemopatrilat and Radioactivity. The mean plasma concentration versus time profiles of gemopatrilat and radioactivity are shown in Fig. 2. Gemopatrilat doses were rapidly absorbed, and the concentrations of radioactivity were substantially higher than unchanged gemopatrilat in human. After the completion of absorption phase, concentrations of gemopatrilat declined rapidly. Within 4 to 5 h after dose, the mean concentrations of gemopatrilat were less than 1% of the mean C_{max} values. In individual subjects receiving 50-mg oral and 20-mg intravenous doses, the plasma concentrations of gemopatrilat were less than 1 ng/ml within 12 to 24 h after dose and declined at a very slow rate thereafter. The postinfusion concentration versus time profiles of gemopatrilat after intravenous doses were curvilinear on a logarithmic ordinate, suggesting multicompartmental pharmacokinetics of gemopatrilat in humans. The initial decline of radioactivity concentrations seemed to be slower than that for unchanged gemopatrilat. Throughout the time course of pharmacokinetic observations after dose, the plasma concentrations of radioactivity were substantially higher compared with unchanged gemopatrilat. Individual pharmacokinetic parameters, determined by a noncompartmental method, are summarized by treatment in Table 1.

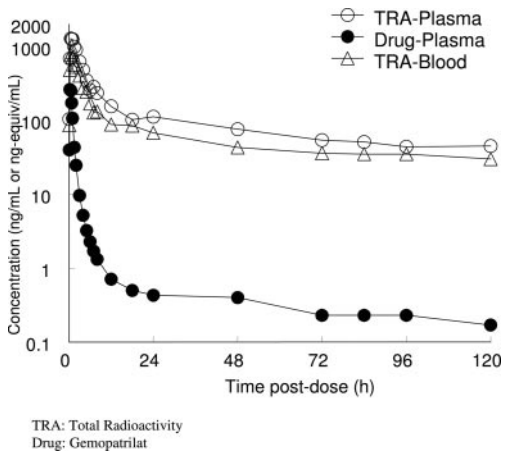

FIG. 2. Blood or plasma concentration versus time profiles for total radioactivity (TRA) and plasma concentration versus time profiles for unchanged gemopatrilat (Drug) in humans after an oral administration of [^{14}C]gemopatrilat. Unchanged gemopatrilat, not bound to plasma thiols via disulfide bond, was measured as the methyl acrylate adduct. The radioactivity, expressed as nanogram-equivalent of gemopatrilat, was measured by liquid scintillation counting and corresponds to gemopatrilat (both free thiol and disulfide forms) and its metabolites.

Radioactivity Elimination Profile. The urinary and fecal excretion of radioactivity in rats, dogs, and humans after oral doses of [^{14}C]gemopatrilat is summarized in Table 2. Radioactivity excreted in the urine and feces for all three species was between 13 to 58% and 18 to 68%, respectively.

Biotransformation Profiles in Plasma. Biotransformation profiles of the methanol extracts of plasma with and without DTT treatment from rat, dog, and human at 1 h after single oral doses of [^{14}C]gemopatrilat are shown in Fig. 3. The recovery of plasma radioactivity into methanol after treatment with DTT was greater than 97% for all three species. The metabolites in the plasma were identified based on the retention times of the standards that were cochromatographed with the samples. The biotransformation profiles of the 6-h plasma samples from rat, dog, and human were qualitatively similar to the 1-h plasma profiles (data not shown).

Rat. In rat 1-h plasma, the methanol extractable radioactivity was 54% before DTT reduction. The prominent metabolites in the non-DTT reduced 1-h rat plasma were M1, M2, and M13, which together accounted for 40% of the radioactivity (Fig. 3). Based on the retention times of the standards, M1, M2, and M13 were identified as the amine-side chain hydrolysis product of gemopatrilat, the *N*-acetylation product of the amine-side chain hydrolysis product of gemopatrilat, and *S*-methyl gemopatrilat, respectively. Minor metabolites present before DTT reduction were M3, M4, M7, M8, M10, M11, and M14, each accounting for 1 to 3% of the radioactivity. The majority of unextractable radioactivity in plasma was characterized after DTT reduction to be gemopatrilat (M12), apparently bound to sulfhydryl groups of plasma proteins by reversible disulfide bonds.

Dog. In 1-h dog plasma samples, the methanol extractable radioactivity was 55% before DTT reduction. The prominent metabolites in the 1-h dog plasma before DTT reduction were M1, M2, M13, and M14, which together accounted for 37% of the radioactivity (Fig. 3). Metabolites M9 and M10, which were not well resolved, accounted for 9% of the radioactivity. The identities of these metabolites were based on the retention times of the standards. Based on the retention

TABLE 1

Pharmacokinetic parameter values for gemopatrilat and radioactivity in human plasma or blood

Treatment/Matrix	C_{max}[a]	T_{max}[b]	AUC(0-T)[a]	AUC(INF)[a]	F[a]	CLT[a]	VSS[a]	MRT[a]	T-HALF[c]
	ng/ml	*h*	*ng h/ml*	*ng h/ml*	*%*	*l/h*	*l*	*h*	*h*
Gemopatrilat									
i.v./plasma	341	0.5	240	268		74	2579	35	130
	(24)	(0.5–0.5)	(29)	(27)		(22)	(81)	(83)	(75)
p.o./plasma	322	0.5	293	314	49			21	88
	(42)	(0.3–0.8)	(32)	(33)	(18)			(81)	(50)
Radioactivity									
p.o./blood	857	0.6	7487	11139					99
	(31)	(0.5–1.5)	(37)	(62)					(46)
p.o./plasma	1362	0.5	11161	15519					85
	(47)	(0.5–1.0)	(56)	(47)					(28)

i.v./plasma, 20-mg gemopatrilat i.v.; p.o./plasma, 50-mg [^{14}C]gemopatrilat oral.
[a] Geometric means (%CV).
[b] Median (minimum–maximum).
[c] Arithmetic mean (S.D.).

TABLE 2

Recovery of radioactivity in urine and feces of rat, dog, and human after an oral dose of [^{14}C]gemopatrilat

Species	Duration	Recovery of Radioactivity (S.D.) as Percent of Dose		
		Urine	Feces	Urine + Feces
Rat[b]	0–24 h	13.3 (5.9)	68.3 (12.9)	81.5 (7.0)
Dog[b]	0–48 h	36.6, 27.6	17.4, 32.5	54.0, 60.2
Human	0–168 h	58.6 (10.1)	18.7 (9.8)	77.3 (13.5)

S.D., standard deviation. Standard deviation is not reported for dog since only two dogs were used; instead, the individual dog recoveries are reported.
[b] The studies were not run as balance studies. The rat and dog samples were only collected for 24 and 48 h, respectively.

times of the standard, M14 was identified as the disulfide of gemopatrilat. Metabolite M9 was determined to be the acyl glucuronide of *S*-methyl gemopatrilat by comparing the retention time with a peak identified by LC/MS and LC/MS/MS in the urine (Fig. 4) and by comparing the retention time with the peak identified in human urine by β-glucuronidase hydrolysis (Fig. 5). The majority of unextractable radioactivity in plasma was characterized after DTT reduction to be gemopatrilat (M12), apparently bound to sulfhydryl groups of plasma proteins by reversible disulfide bonds.

Human. In 1-h human plasma samples, the methanol extractable radioactivity before DTT reduction was 50%. The prominent metabolites in the 1-h human plasma before DTT reduction were M2, M13, and M14, which together accounted for 31% of the radioactivity (Fig. 3). Metabolites M9 and M10, which were not well resolved, accounted for 8% of the radioactivity. Minor components present in 1- and 6-h plasma samples before DTT reduction were M4, M6 to M8, M11, and M12 (gemopatrilat) each accounting for 1 to 3% of the radioactivity. The identities of these metabolites were based on the retention times of the standards. The majority of unextractable radioactivity in plasma was characterized after DTT reduction to be gemopatrilat (M12), apparently bound to sulfhydryl groups of plasma proteins by reversible disulfide bonds.

Species Comparison of Biotransformation Profiles in Urine and Feces. The biotransformation profiles of pooled urine and feces from rat (0–24 h), dog (0–48 h), and human (0–168 h) after single oral doses of [^{14}C]gemopatrilat are shown in Fig. 4.

Rat. Rats excreted an average of 13% of the radioactive dose in urine over a period of 24 h. No parent compound was detected in the urine. The prominent metabolites were M1, M4, and M13, which individually accounted for 19 to 27% of the radioactivity and together accounted for 69% of the radioactivity (Fig. 4). Metabolites M3, M7, and M8, which individually accounted for 6 to 10% of the radioactivity, together accounted for 16% of the radioactivity. Metabolites M6 and M14 accounted for 2 and 3% of the radioactivity, respectively. All other metabolites accounted for less than 1% of the radioactivity. Metabolites M3 and M4 were identified as the diastereomers of the *S*-methyl sulfoxide of the acid-side hydrolysis product of gemopatrilat. Metabolites M7 and M8 were identified as the diastereomers of *S*-methyl gemopatrilat sulfoxide. The identities of these metabolites were based both on the retention times and LC/MS/MS fragmentation patterns that were similar to that of the synthetic standards (Table 3). Metabolite M9, which was identified as the glucuronic acid conjugate of *S*-methyl gemopatrilat, showed the characteristic loss of *m/z* 176 (−glucuronide) in the LC/MS/MS analysis mode. The nine metabolites identified in the rat urine accounted for 91% of the urinary radioactivity.

Rats excreted an average of 68% of the radioactive dose in feces over a period of 24 h. No parent compound was detected in the feces. The prominent metabolites were M13 and M14, which accounted for 70 and 14% of the radioactivity, respectively (Fig. 4). Metabolites M7 and M8 accounted for 7% of the radioactivity, and M10 accounted for 2% of the radioactivity. The identities of these metabolites were based both on the retention times and LC/MS/MS fragmentation patterns that were similar to that of the synthetic standards (Table 3). The metabolites identified in the rat feces accounted for 93% of the fecal radioactivity.

Dog. The two individual dogs excreted 28 and 37% of the radioactive dose in urine over a period of 48 h. No parent compound was detected in the urine. The metabolites detected were M1, M2, M4 to M9, M13, and M14 (Fig. 4). The most prominent metabolite was M13, which accounted for 47% of the radioactivity. Metabolites M1, M4 to M9, and M14, which individually accounted for 5 to 10% of the radioactivity, together accounted for 46% of the radioactivity. The identities of these metabolites were based both on the retention times and LC/MS/MS fragmentation patterns that were similar to that of the synthetic standards (Table 3). Metabolites M5 and M9 were determined to be the acyl glucuronides of the cysteine disulfide of gemopatrilat and the *S*-methyl gemopatrilat, respectively, based on the loss of *m/z* 176 (−glucuronide) in the LC/MS/MS analysis mode. The 10 metabolites identified in dog urine accounted for 93% of the urinary radioactivity.

The two individual dogs excreted 17 and 33% of the radioactive dose in feces over a period of 48 h. No parent compound was detected in the feces. The metabolites detected were M1, M2, M4, M6 to M8, M10, M11, M13, and M14 (Fig. 4). The most prominent metabolite was M13, which accounted for 54% of the radioactivity. Metabolites M1, M2, M7, M8, M11, and M14, which individually accounted for

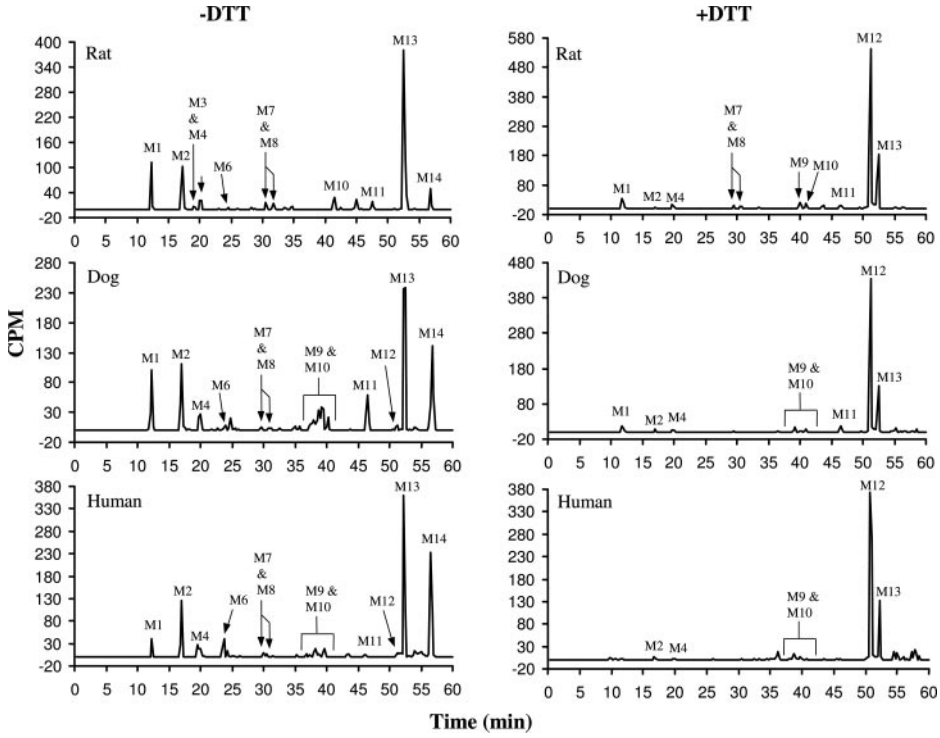

FIG. 3. Biotransformation profiles of 1-h pooled rat, dog, and human plasma before (−DTT) and after DTT treatment. The plasma samples were obtained after oral administration of [^{14}C]gemopatrilat to rat (50 mg/kg), dog (100 mg), and human (50 mg). The profiles are a background-subtracted reconstructed radiochromatogram of 15-s fractions collected from a HPLC run.

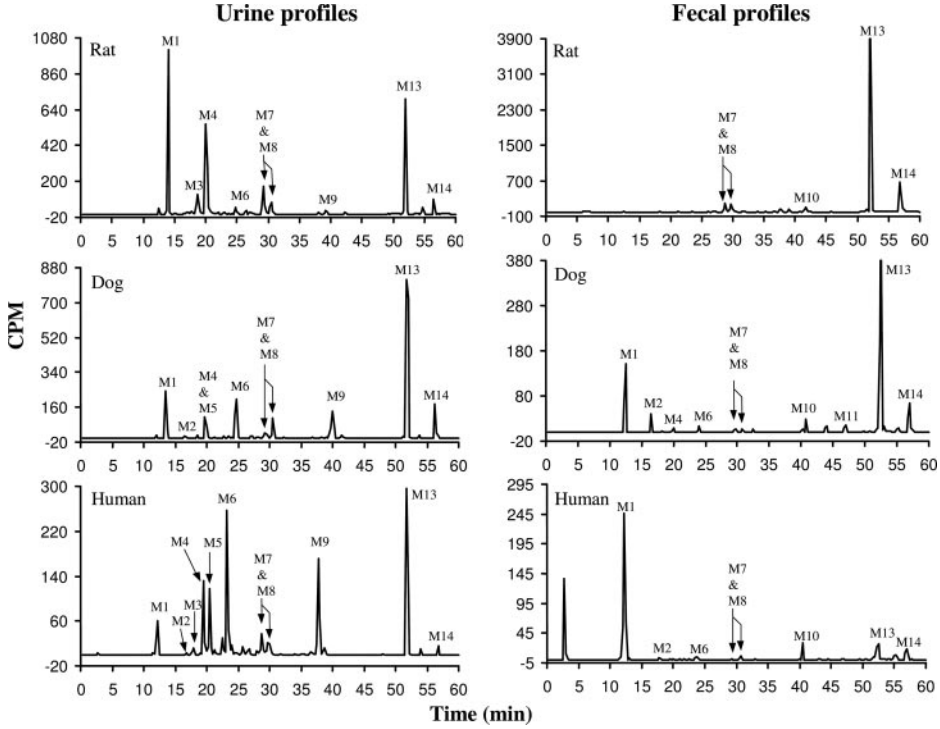

FIG. 4. Biotransformation profiles of pooled urine and fecal samples after oral administration of [^{14}C]gemopatrilat to rat (50 mg/kg), dog (100 mg), and human (50 mg). The pooling intervals for these samples were 0 to 24, 0 to 48, and 0 to 168 h for rat, dog, and human, respectively. The profiles are a background-subtracted reconstructed radiochromatogram of 15-s fractions collected from a HPLC run.

2 to 18% of the radioactivity, together accounted for 34% of the radioactivity. All other metabolites accounted for less than 2% of the radioactivity. The identities of these metabolites were based on the retention times of the standards. The identity of the metabolites M6 to M8, M13, and M14 were further confirmed by LC/MS/MS analysis, where their fragmentation patterns observed were similar to those of the respective synthetic standards. The 10 metabolites identified in dog feces accounted for 92% of the fecal radioactivity.

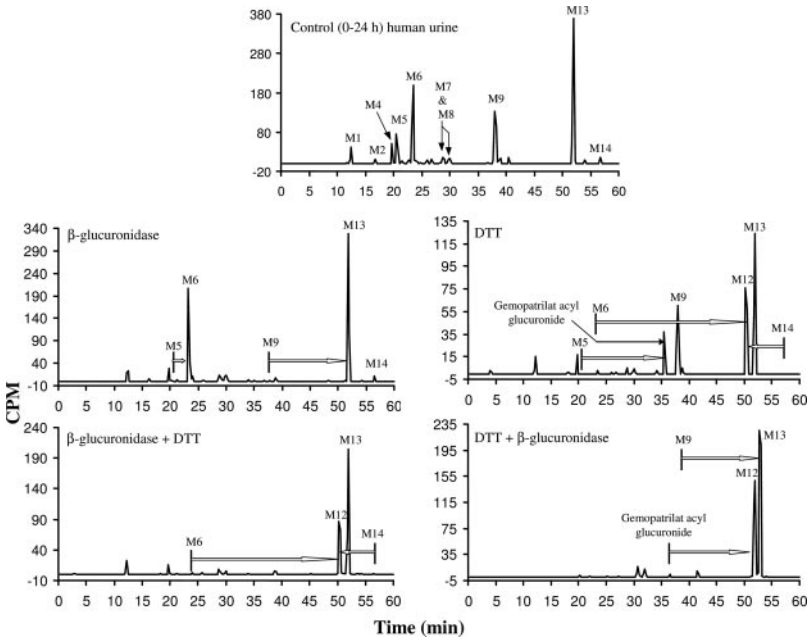

FIG. 5. Biotransformation profiles of pooled 0 to 24-h human urine before and after β-glucuronidase, β-glucuronidase + DTT, DTT, or DTT + β-glucuronidase treatments. The profiles are a background-subtracted reconstructed radiochromatogram of 15-s fractions collected from a HPLC run.

TABLE 3

LC/MS/MS analysis of gemopatrilat and its metabolites detected in urine and feces of rat, dog, and human

Metabolite[a]	Matrix/Species[b]	Negative Ion Electrospray Ionization
		Relevant ions m/z (loss of fragment)
M3 and M4[c]	Urine: R, D	MS: 211 (M-H); MS^2 on 211: 63 (M-148, CH_3SO), 81 (M-130, $CH_3SO + H_2O$)
M5	Urine: D, H	MS: 672 (M-H); MS^2 on 672: 551 (M-121, -cysteine), 496 (M-176, -glucuronide), 375 (M-297, -cysteine, and -glucuronide)
M6	Urine: R, D, H Feces: D	MS: 496 (M-H); MS^2 on 496: 375 (M-121, -cysteine)
M7 and M8[d]	Urine: R, D, H Feces: R, D	MS: 407 (M-H); MS^2 on 407: 343 (M-64, $-CH_3S(O)H$), 188 (M-219, $C_{11}H_{10}N_1O_2$)
M9	Urine: R, D, H	MS: 567 (M-H); MS^2 on 567: 391 (M-176, -glucuronide), 343 (M-224, -glucuronide, and $-CH_3S$), 188 (M-379, $C_{11}H_{10}N_1O_2$)
M13	Urine: R, D, H Feces: R, D	MS: 391 (M-H); MS^2 on 391: 343 (M-48, $-CH_3S$), 188 (M-203, $C_{11}H_{10}N_1O_2$)
M14	Urine: R, D, H Feces: R, D	MS: 754 (M-H); MS^2 on 754: 375 (M-379, $-C_{19}H_{26}N_2O_4S$)

[a] Metabolites M1 and M2 were not identified by LC/MS or LC/MS/MS because of poor ionization.
[b] R, D, and H represent rat, dog, and human, respectively.
[c] Diastereomeric sulfoxides of M11. Metabolites M3 and M4 had different retention times on the HPLC and were analyzed separately.
[d] Diastereomeric sulfoxides of M13. Metabolites M7 and M8 had different retention times on the HPLC and were analyzed separately.

Human. Humans excreted an average of 59% of the radioactive dose in the urine over a period of 168 h. No parent compound was detected in the urine. The metabolites detected were M1 to M9, M13, and M14 (Fig. 4). The prominent metabolites were M4–M6, M9, and M13, which individually accounted for 8 to 24% of the radioactivity and together accounted for 75% of the radioactivity. Metabolites M1, M3, M7, and M8, which individually accounted for 1 to 7% of the radioactivity, together accounted for 14% of the radioactivity. The identities of these metabolites were based on the retention times of the standards and were further confirmed by LC/MS/MS analysis, where the fragmentation pattern observed was similar to that of the synthetic standards (Table 3).

In addition, pooled human (0–24 h) urine was treated with β-glucuronidase/sulfatase and dithiothreitol sequentially to determine the identities of M5 and M9. The urine profile after hydrolysis with β-glucuronidase/sulfatase (Fig. 5) showed the disappearance of peaks M5 and M9 and an increase in the radioactivity of M6 and M13, which are the cysteine disulfide of gemopatrilat and *S*-methyl gemopatrilat, respectively. Incubation in the presence of 1,4-saccharolactone, a β-glucuronidase inhibitor, prevented the hydrolysis of M5 and M9 (data not shown), showing that these metabolites are β-glucuronic acid conjugates. The β-glucuronidase-treated urine was also reduced with DTT, which showed the disappearance of peak M6 and the appearance of peak M12, which is gemopatrilat (Fig. 5). These experiments indicated that M5 and M9 were acyl glucuronides of cysteine disulfide of gemopatrilat and *S*-methyl gemopatrilat, respectively.

To further confirm the identity of M5, the 0 to 24-h pooled urine was also reduced with DTT without prior β-glucuronidase hydrolysis. The urine profile after DTT reduction showed the disappearance of M5 and the appearance of a peak at 36 min (Fig. 5). After hydrolysis with β-glucuronidase, the 36-min peak disappeared, and the radioactivity of gemopatrilat increased. This experiment confirmed the finding that metabolite M5 was the acyl glucuronide of cysteine disulfide of gemopatrilat. The 11 metabolites identified in human urine accounted for 90% of the urinary radioactivity.

Humans excreted an average of 19% of the radioactive dose in the feces over a period of 168 h. No parent compound was detected in the feces. The metabolites detected were M1, M2, M6 to M8, M10, M13,

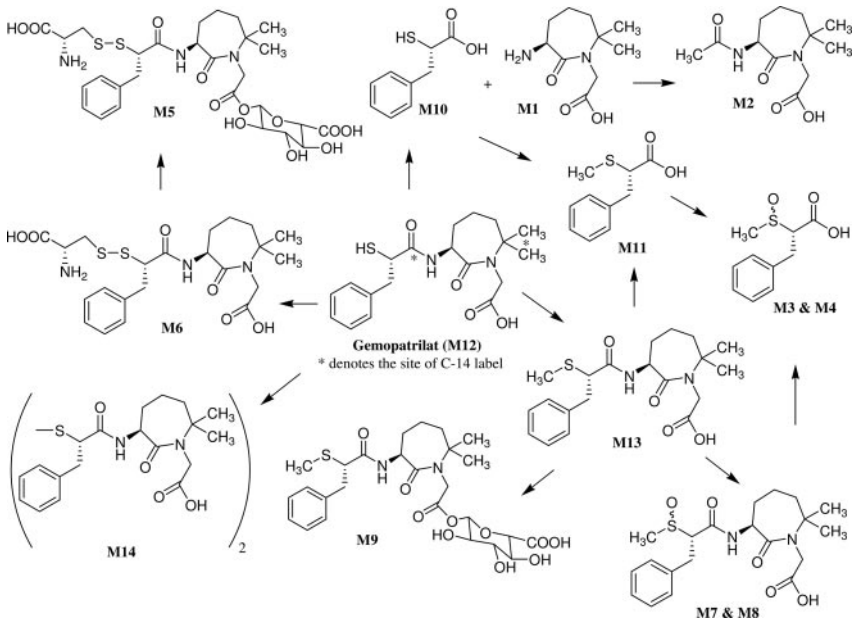

FIG. 6. Proposed biotransformation pathways for gemopatrilat based on metabolites identified in plasma, urine, and fecal samples from rat, dog, and human administered a single oral dose of [^{14}C]gemopatrilat.

and M14 (Fig. 4). The prominent metabolite was M1, which accounted for 52% of the radioactivity. Metabolites M10, M13, and M14, which individually accounted for 4 to 9% of the radioactivity, together accounted for 18% of the radioactivity. The identities of these metabolites were based on the retention times of the standards. One unidentified peak eluting at the void volume accounted for 21% of the radioactivity in the human feces. This void volume peak accounts for only 3.9% of the total radioactive dose. It is possible that this peak contains more than one polar metabolite, which may have formed as a result of biotransformation by the gut microflora. This peak was not further identified. The eight metabolites identified in human feces accounted for 74% of the fecal radioactivity.

Discussion

The proposed pathway for biotransformation of gemopatrilat in humans is shown in Fig. 6. The pathway is based on the biotransformation profiles in plasma, urine, and feces of rat, dog, and human. The primary pathways responsible for metabolism of gemopatrilat were *S*-methylation, amide hydrolysis, and disulfide formation. Sulfoxidation and glucuronidation of the *S*-methylated metabolites of gemopatrilat were identified as secondary pathways of metabolism. Amide hydrolysis, resulting in the formation of (*S*)-2-thio-3-phenylpropionic acid, was shown to be one of the major metabolic pathways for omapatrilat (Iyer et al., 2001, 2003), and given the similarity of omapatrilat with gemopatrilat, the same would be expected for the latter. Therefore, the radioactivity studies of these two compounds with a single [^{14}C] label would not elucidate the metabolic fate of the complete molecule. Based on this consideration, the current study was conducted with a mixture of [^{14}C]-labeled gemopatrilat: one [^{14}C] label at the exocyclic carbonyl carbon and the other [^{14}C] label on one of the carbons of the gem-dimethyl group (Fig. 1). The radioactivity-excretion data and the biotransformation profiles in this study of [^{14}C]-labeled gemopatrilat would be representative of gemopatrilat and its metabolites, including those formed after hydrolysis of the amide bond.

Pharmacokinetics of Gemopatrilat in Humans. The maximum plasma concentrations of gemopatrilat occurred within 15 to 45 min after oral dosing, suggesting rapid oral absorption. The absolute bioavailability of gemopatrilat given orally as a solution, was approximately 49%, suggesting substantial presystemic first-pass metabolism and possibly incomplete oral absorption.

Compounds such as omapatrilat and captopril, which contain a free sulfhydryl group have the propensity to form disulfide linkages with endogenous thiols, including cysteine and the thiols on proteins (Kripalani et al., 1983; Migdalof et al., 1984; Iyer et al., 2001; Malhotra et al., 2001). Approximately half of the drug-related radioactivity in the systemic circulation was present as disulfide forms of gemopatrilat and its sulfhydryl-containing metabolites that was not extractable into organic solvents but could be reduced chemically to gemopatrilat and its sulfhydryl-containing metabolites ex vivo after treatment of plasma with dithiothreitol, a disulfide-reducing agent (Fig. 3). It is, therefore, possible that a fraction of the gemopatrilat dose may be bound to the plasma and tissue proteins via slowly reversible disulfide linkages and would be eliminated from the body at a very slow rate according to the turnover rate of the proteins. The slow decline in the plasma concentrations of radioactivity, with a terminal half-life of approximately 4 days, is also suggestive of this possibility. The prolonged terminal-phase decline in the plasma concentrations of radioactivity and gemopatrilat appeared to be parallel, with a half-life of 88 and 81 h, respectively (Fig. 2). The apparent steady-state volume of distribution of gemopatrilat, averaging approximately 2500 liters, was high compared with the total body water of approximately 42 liters and is probably related to extravascular distribution of gemopatrilat and also formation of disulfide linkages with the thiols of circulating macromolecules. Based on a comparison of the AUC(INF) values, unchanged gemopatrilat represented approximately 2% of the radioactivity in plasma, indicating that a majority of the radioactivity in systemic circulation represents the metabolites and disulfide conjugates of gemopatrilat.

In humans, the radioactivity administered orally as [^{14}C]gemopatrilat was eliminated primarily in the urine (59% of the dose). The total recovery of radioactivity in the urine and feces, collected over 168 h after a single oral dose of [^{14}C]gemopatrilat, averaged 77% and ranged between 53 and 91% of the administered dose. Although the

reason for incomplete recovery of radioactivity is not entirely clear, possible incomplete collection of the excreta may in part be responsible. The total body clearance of gemopatrilat averaged approximately 74 l/h and was greater than the liver plasma flow (50 l/h), indicating that extrahepatic organs may be involved in the elimination of gemopatrilat.

Comparative Biotransformation Profiles of Gemopatrilat in Rat, Dog, and Human. In this study, comparative metabolic profiles were generated to evaluate the exposure of gemopatrilat and its metabolites in rats, dogs, and humans after oral administration of [^{14}C]gemopatrilat. Rats and dogs were chosen for comparison because they were the species used in long-term toxicity studies during the development of the compound.

The major metabolites in human plasma formed through *S*-methylation, amide hydrolysis, and disulfide formation were also present in dog and rat plasma. There was very little parent compound present in the extracted sample. The metabolites identified in the extracted sample, except for metabolites M1, M2, and M14, were all derived from *S*-methyl gemopatrilat. These results suggest that the metabolic pathways in vivo for gemopatrilat are similar in rats, dogs, and humans. The circulating metabolites identified are all expected to be inactive toward ACE and NEP because of the absence of the free sulfhydryl group, which is necessary for coordinating with the zinc atom in the active site of both the enzymes (Delaney et al., 1994).

A portion of the radioactivity was unextractable in 1-h plasma sample from all three species. After DTT reduction of plasma, the recovery of radioactivity was quantitative for all three species. Gemopatrilat and (*S*)-2-thio-3-phenylpropionic acid accounted for the majority of the radioactivity recovered upon DTT treatment. Because both of these compounds are sulfhydryl-containing compounds, they were probably bound to the plasma protein via disulfide bonds. The presence of very little parent compound in the 1-h plasma sample before DTT reduction in all three species suggested that unchanged gemopatrilat was rapidly cleared from the plasma by forming disulfide linkages with cysteine sulfhydryl groups on the protein. This phenomenon has been observed for other sulfhydryl containing compounds like omapatrilat, captopril, and penicillamine (Kripalani et al., 1983; Migdalof et al., 1984; Keire et al., 1993; Iyer et al., 2001; Malhotra et al., 2001). Due to the reversible nature of the disulfide bond in vivo (Gilbert, 1995), the disulfide adducts of gemopatrilat could act as depot for slow release of the drug.

No gemopatrilat was detected in urine and fecal samples from all three species, suggesting that the compound is extensively metabolized in vivo before being eliminated. The major metabolites identified in rat, dog, and human urine were the hydrolysis product of gemopatrilat, namely the amine (M1), the sulfoxide of (*S*)-2-thiomethyl-3-phenylpropionic acid (M4), and *S*-methyl gemopatrilat (M13). In addition, in dog and human urine, the acyl glucuronide (M9) and cysteine disulfide adduct (M6) and its acyl glucuronide (M5) were also identified as major metabolites. In rat feces, *S*-methyl gemopatrilat (M13) was the major metabolite detected, whereas in human feces the amine-side hydrolysis product M1 was the major metabolite identified. In dog, both M1 and M13 were identified as the major metabolites. These results seem to suggest that although the metabolism profiles across species were similar, there are significant differences as to the routes of elimination of metabolites. *S*-Methyl gemopatrilat and its acyl glucuronide were detected as major metabolites in rat bile (R. A. Iyer and J. Mitroka, personal communication). The absence of the acyl glucuronide (M9) in fecal samples is probably due to the hydrolysis by the glucuronidases present in the gut wall and in the intestinal microflora. The different routes of excretion for the hydrolysis products of gemopatrilat (molecular mass $<$300 Da) compared with the metabolites of *S*-methyl gemopatrilat (molecular mass $>$325 Da) in rat may be due to the molecular mass cut-off of 325 $\pm$ 50 Da for excretion into the bile (Klaassen et al., 1981).

Although the primary pathways of metabolism between omapatrilat and gemopatrilat, namely *S*-methylation, amide hydrolysis, and disulfide formation, were similar, there are important differences between the metabolism of two compounds. These arise because of the differences in the chemical structure of the amine portion of the molecule. For gemopatrilat, two metabolites, the acyl glucuronide of the cysteine-disulfide adduct and the *N*-acetyl derivative of the amine hydrolysis product, were unique metabolites and were not observed for omapatrilat. For omapatrilat, which has an additional sulfur in the ring, sulfoxide metabolites of the ring sulfur were observed in vivo (Iyer et al., 2001, 2003). Gemopatrilat does not have additional ring sulfur to undergo similar metabolism.

In conclusion, gemopatrilat is extensively metabolized in all three species, and the systemic exposure to the metabolites in rat, dog, and human were qualitatively very similar. All the metabolites that were identified, except for the L-cysteine-mixed disulfide and the symmetrical disulfide that could potentially be reduced to gemopatrilat in vivo, are expected to be inactive toward ACE and NEP. Finally, this article extends the strategy of using dual-labeled material to understand the complete metabolism of a compound. This is a useful approach to use where metabolism could spilt the molecule by half, and having a dual label helps to follow the fate of both sides of the molecule.

Acknowledgments. We thank the Clinical Pharmacology Unit of Clinical Discovery Department, Bristol-Myers Squibb Pharmaceutical Research Institute, Hamilton, NJ for providing the human plasma and urine samples from their study with [^{14}C]gemopatrilat. We also thank the Technical Support Unit of Preclinical Lead Optimization Department, Bristol-Myers Squibb Pharmaceutical Research Institute, Princeton, NJ for conducting the studies in rat and dog with [^{14}C]gemopatrilat.

References

Burnett JCJ (1999) Vasopeptidase inhibition: a new concept in blood pressure management. *J Hypertens* **17 (Suppl 1):**S37–S43.

Delaney NG, Barrish JC, Neubeck R, Natarajan S, Cohen M, Rovnyak GC, Huber G, Murugesan N, Girotra R, Sieber-McMaster E, et al. (1994) Mercaptoacyl dipeptides as dual inhibitors of angiotensin-converting enzyme and neutral endopeptidase. Preliminary structure-activity studies. *Bioorg Med Chem Lett* **4:**1783–1788.

Gilbert HF (1995) Thiol/disulfide exchange equilibria and disulfide bond stability. *Meth Enzymol* **251:**8–28.

Hubner RA, Kubota E, Casley DJ, Johnston CI, and Burrell LM (2001) In-vitro and in-vivo inhibition of rat neutral endopeptidase and angiotensin converting enzyme with the vasopeptidase inhibitor gemopatrilat. *J Hypertens* **19:**941–946.

Iyer RA, Malhotra B, Mitroka J, Khan S, Bonacorsi S Jr, Waller SC, Rinehart JK, and Kripalani K (2003) Comparative biotransformation of radiolabeled [^{14}C]omapatrilat and stable-labeled [$^{13}C_2$]omapatrilat after oral administration to rats, dogs and humans. *Drug Metab Dispos* **31:**67–75.

Iyer RA, Mitroka J, Malhotra B, Bonacorsi S Jr, Waller SC, Rinehart JK, Roongta VA, and Kripalani K (2001) Metabolism of [^{14}C]omapatrilat, a sulfhydryl-containing vasopeptidase inhibitor in humans. *Drug Metab Dispos* **29:**60–69.

Jemal M and Hawthorne DJ (1997a) Quantitative determination of BMS-186716, a thiol compound, in dog plasma by high-performance liquid chromatography-positive ion electrospray mass spectrometry after formation of the methyl acrylate adduct. *J Chromatogr Biomed Appl* **693:**109–116.

Jemal M and Hawthorne DJ (1997b) Quantitative determination of BMS-186716, a thiol compound, in rat plasma by high-performance liquid chromatography-positive ion electrospray mass spectrometry after hydrolysis of the methyl acrylate adduct by the native esterases. *J Chromatogr Biomed Appl* **698:**123–132.

Jemal M, Khan S, Teitz DS, McCafferty JA, and Hawthorne DJ (2001) LC/MS/MS determination of omapatrilat, a sulfhydryl-containing vasopeptidase inhibitor and its sulfhydryl- and thioether-containing metabolites in human plasma. *Anal Chem* **73:**5450–5456.

Keire DA, Mariappan SV, Peng J, and Rabenstein DL (1993) Nuclear magnetic resonance studies of the binding of captopril and penicillamine by serum albumin. *Biochem Pharmacol* **46:** 1059–1069.

Klaassen CD, Eaton DL, and Cagen SZ (1981) Hepatobiliary disposition of xenobiotics, in *Progress in Drug Metabolism* (Bridges JW and Chasseaud LF eds) pp 1–75, John Wiley & Sons Ltd, New York.

Kripalani KJ, Dean AV, and Migdalof BH (1983) Metabolism of captopril-L-cysteine, a captopril metabolite, in rats and dogs. *Xenobiotica* **13:**701–705.
Malhotra BK, Iyer RA, Soucek KM, Behr D, Liao WC, Mitroka J, Kaul S, Cohen MB, and Knupp CA (2001) Oral bioavailability and disposition of [14C]omapatrilat in healthy subjects. *J Clin Pharmacol* **41:**833–841.
Migdalof BH, Antonaccio MJ, McKinstry DN, Singhvi SM, Lan S-J, Egli P, and Kripalani K (1984) Captopril: pharmacology, metabolism and disposition. *Drug Metab Rev* **15:**841–869.
Robl JA, Sulsky R, Sieber-McMaster E, Ryono DE, Cimarusti MP, Simpkins LM, Karanewsky DS, Chao S, Asaad MM, Seymour AA, et al. (1999) Vasopeptidase inhibitors: incorporation of geminal and spirocyclic substituted azepinones in mercaptoacyl dipeptides. *J Med Chem* **42:**305–311.
Sagnella GA (2002) Vasopeptidase inhibitors. *J Renin Angiotensin Aldosterone Syst* **3:**90–95.
Seymour AA, Abboa-Offei BE, Smith PL, Mathers PD, Asaad MM, and Rogers WL (1995) Potentiation of natriuretic peptides by neutral endopeptidase inhibitors. *Clin Exp Pharmacol Physiol* **22:**63–69.
Singh J, Kronenthal DR, Schwinden M, Godfrey JD, Fox R, Vawter EJ, Zhang B, Kissick TP, Patel B, Mneimne O, et al. (2003) Efficient asymmetric synthesis of the vasopeptidase inhibitor BMS-189921. *Org Lett* **5:**3155–3158.
Trippodo NC, Panchal BC, and Fox M (1995) Repression of angiotensin II and potential of bradykinin contribute to the synergistic effects of dual metalloprotease inhibition in heart failure. *J Pharmacol Exp Ther* **272:**619–627.
Yang D, Li B, Ng F, Yan Y, Qu J, and Wu Y (2001) Synthesis and characterization of chiral N-O turns induced by α-aminoxy acids. *J Org Chem* **66:**7303–7312.

Address correspondence to: Dr. Ramaswamy A. Iyer, Department of Biotransformation, Bristol-Myers Squibb Pharmaceutical Research Institute, P.O. Box 4000, Mail Stop F13-01, Princeton, NJ 08540. E-mail: ramaswamy.iyer@bms.com